Transport and electronic properties of $DyRu_2Si_2$ and $ErRu_2Si_2$ compounds

1999 J. Phys.: Condens. Matter 11 8069

(http://iopscience.iop.org/0953-8984/11/41/310)

J. Phys.: Condens. Matter **11** (1999) 8069–8079. Printed in the UK PII: S0953-8984(99)02281-X

Transport and electronic properties of $DyRu_2Si_2$ and $ErRu_2Si_2$ compounds

J Budzioch†, A Jezierski‡, V Ivanov§, B Penc† and A Szytuła†‖

† Institute of Physics, Jagiellonian University, Reymonta 4, 30-059 Kraków, Poland
‡ Institute of Molecular Physics, Polish Academy of Sciences, Smoluchowskiego 17, 60-179 Poznań, Poland
§ General Physics Institute, Academy of Sciences, 117942 Moscow, Russian Federation

E-mail: szytula@if.uj.edu.pl

Received 3 March 1999, in final form 14 June 1999

Abstract. Results of the transport and electronic structure of $DyRu_2Si_2$ and $ErRu_2Si_2$ compounds are presented. These compounds crystallize in a tetragonal $ThCr_2Si_2$-type of structure. At high temperatures the resistivity varies linearly with temperature, whereas at low temperatures anomalies connected with the magnetic phase transitions are observed. The electronic structure and corresponding x-ray photoemission spectra (XPS) are presented. The band structure is calculated by the spin-polarized tight-binding linear muffin-tin orbital (TB LMTO) method. The XPS valence bands are compared with the calculated electronic density of states. In both compounds 4d states of Ru atoms form a band near to the Fermi level.

1. Introduction

The ternary rare earth silicides RRu_2Si_2 (R = rare earth metal) crystallize in the $ThCr_2Si_2$ ($CeAl_2Ge_2$) type of structure. These compounds usually order magnetically at low temperatures. For the R = Tb–Er compounds below the Néel temperature a sine modulated magnetic ordering is observed [1]. For $DyRu_2Si_2$ the following temperature behaviour is observed at low temperatures:

- the specific heat exhibits an anomaly at $T_t \sim 1.5$ and 3.5 K [2];
- the magnetization curve reveals metamagnetic transitions in $H \sim 1.8$ kOe and 9 K at $T = 1.5$ K and in $H = 10$, 15.5 and 17.5 kOe at $T = 4.2$ K [2];
- neutron diffraction data indicate a complete antiphase structure below 5 K [3].

The magnetic (H, T) phase diagram for $DyRu_2Si_2$ was presented by Andreani *et al* [4]).

For the $ErRu_2Si_2$ compound the sine modulated structure is stable in temperature region from 1.5 up to $T_N = 6$ K [5] and the magnetic field induces the one-step metamagnetic process [6].

In this work we report the results of electrical resistivity measurements without and with magnetic field H applied up to 12.1 kOe and also experimental and theoretical studies of the electronic structures of $DyRu_2Si_2$ and $ErRu_2Si_2$. The x-ray photoemission spectroscopy (XPS) valence band spectra are compared with *ab initio* electronic structure calculations using the tight-binding linear muffin-tin orbital (TB LMTO) method [7].

‖ Author to whom any correspondence should be addressed.

0953-8984/99/418069+11$30.00

2. Experimental details

The $DyRu_2Si_2$ and $ErRu_2Si_2$ samples were arc melted from the constituent metals in a cooled copper crucible in a high-purity argon atmosphere, remelted several times and then annealed at 800 °C for a week. The phase purity of compounds was checked by the x-ray Debye–Scherrer diffraction with Co Kα radiation using the DRON-3 diffractometer. Both compounds crystallize in the tetragonal structure.

The electrical resistivity R measurements without and with the magnetic field H applied up to 12.1 kOe were carried out in the temperature interval 2–300 K using a conventional four point-probe method.

The XPS spectra were obtained at room temperature using a Specs ESCA spectrometer with Mg Kα ($h\nu = 1253.6$ eV) and Al Kα ($h\nu = 1486.6$ eV) radiation and with a helium discharge lamp for ultraviolet photoemission spectroscopy (He I: $h\nu = 21.2$ eV, He II: $h\nu = 40.8$ eV). The total energy resolution of the spectrometer with a hemispherical energy analyser was about 0.75 eV for Ag 3d with Mg Kα and about 0.8 eV for Ag 3d with Al Kα. Binding energies were referred to the Fermi level ($E_F = 0$).

3. The method of calculation

The electronic structure was calculated by the *ab initio* self-consistent tight-binding linear muffin-tin orbital (TB LMTO) method [7] within the framework of the local spin density approximation (LSD). The scalar-relativistic approximation for band electrons and the fully relativistic treatment of the frozen core electrons were used. The exchange–correlation potential was assumed in the form proposed by von Barth and Hedin [8] and the gradient corrections were included [9]. The self-consistent calculations were performed in the atomic sphere approximation (ASA). The values of the atomic sphere radii S_x (x = Dy, Er, Ru, Si) were chosen in such a way that the sum of all atomic sphere volumes was equal to the volume of the unit cell. Using experimental values of the lattice parameters we obtained the following values of S_x/S_{av} ratio: Dy—1.23, Ru—0.92 and Si—0.93 for $DyRu_2Si_2$ and Er—1.25, Ru—0.94 and Si—0.88 for $ErRu_2Si_2$. For such values of the atomic radii the overlapping of the spheres was less than 10%. In the band calculations the initial atomic configurations were taken according to the periodic table of elements: Dy, $4f^9$; Er, $4f^{11}$; Ru, $4d^75s^1$; Si $3p^23p^2$. The energy was calculated for 349 k-points in the irreducible wedge of the Brillouin zone.

The magnetic moments were calculated by the spin-polarized TB LMTO method. We have applied the scheme proposed by Brooks *et al* [10] in which the 4f states of Dy or Er were treated as open core states. In this model the 4f states of rare earth (R) did not hybridize with the conduction electron states and the number of 4f electrons of R was fixed to be an integer number.

We have also performed the spin-polarized band calculations for the full hybridization of s, p, d and f electrons. The results are presented in section 4.3.

4. Results and discussion

4.1. Electrical resistivity

The electrical-transport properties are very sensitive to the electronic structure as well as the magnetic nature of the materials studied. Intermetallic compounds with 'nd' transition metals are expected to show more complex behaviour because of the itinerant character of the d and

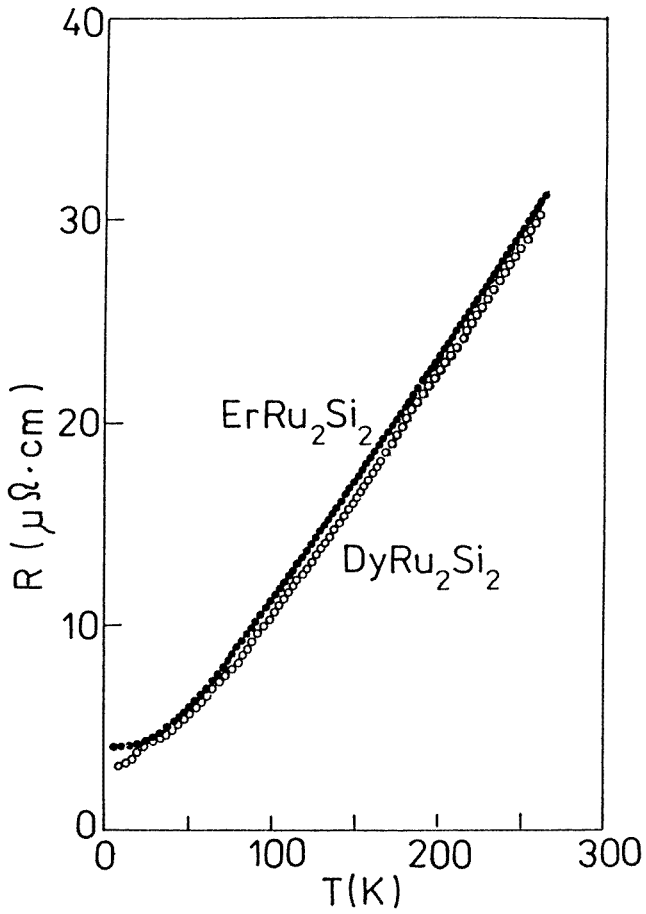

Figure 1. Temperature variation of the electrical resistivity R for $DyRu_2Si_2$ and $ErRu_2Si_2$.

s electrons. According to Matthiessen's rule the total resistivity of a magnetically ordered material can be written as:

$$R(T) = R_0 + R_{ph}(T) + R_{mag}(T) \tag{1}$$

where R_0 is the residual resistivity, $R_{ph}(T)$ is the contribution due to electron–phonon interaction and $R_{mag}(T)$ is the contribution due to electron–spin wave scattering. According to the temperature region, either $R_{ph}(T)$ or $R_{mag}(T)$ predominates.

The temperature dependence of the electric resistivity R of both compounds is shown in figures 1–3. At temperatures above 100 K, the resistivity increases almost linearly with temperature as in normal metals, reaching a value of 32 $\mu\Omega$ cm for $DyRu_2Si_2$ and 34 $\mu\Omega$ cm for $ErRu_2Si_2$ at room temperature. This indicates good quality specimens without significant internal microcracks. The resistivity slope is then $\sim$0.12 $\mu\Omega$ cm K^{-1} for $DyRu_2Si_2$ and 0.10 $\mu\Omega$ cm K^{-1} for $ErRu_2Si_2$. These values suggest that electrical resistivity is dominated by electron–phonon scattering. At low temperatures, anomalies around the Néel temperatures, at 28.5 K for $DyRu_2Si_2$ and 6 K for $ErRu_2Si_2$, are visible. For $DyRu_2Si_2$ an additional minimum of the electrical resistivity at $T = 3.2$ K is observed (figure 2). In the case of $ErRu_2Si_2$

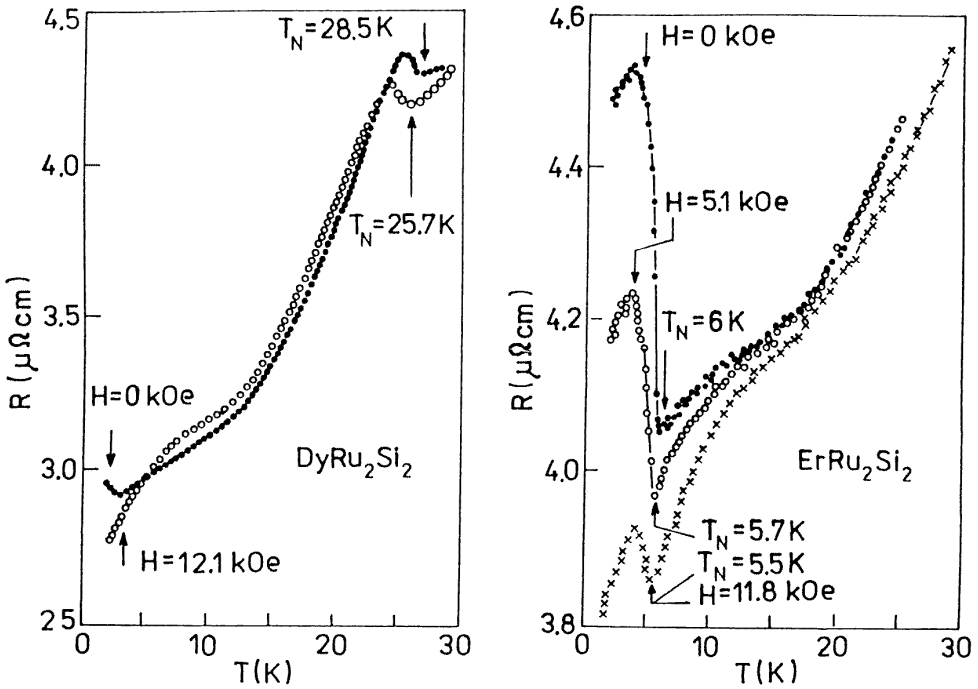

Figure 2. Low temperature part of resistivity of $DyRu_2Si_2$ and $ErRu_2Si_2$ at different magnetic fields.

an anomaly at low temperatures near $T_N = 6$ K is observed (figure 2). Below ~80 K for $DyRu_2Si_2$ and 60 K for $ErRu_2Si_2$, precursor effects of the antiferromagnetic transition are observed, which causes a progressive increase of R, above the phonon term. Initial growth of fluctuations in the paramagnetic phase amplifies the magnetic electron scattering producing negative dR/dT values (figure 3). In both compounds, dR/dT shows marked anomalies at T_N (figure 3). Below T_N, dR/dT of $DyRu_2Si_2$ decreases with an increasing sinusoidal order until 4.6 K where the subsequent increase followed by a rapid decrease is observed. A similar effect is observed in the isostructural $TbRu_2Si_2$ [12]. The increase of dR/dT at low temperatures is associated with the change of the magnetic structure [3].

For $DyRu_2Si_2$, the external magnetic field $H = 12.1$ kOe changes the Néel temperature from 28.5 K to 25.7 K and causes disappearance of the minimum of $R(T)$ at 3.2 K (see figure 2). This result is in accord with the magnetic phase diagram of $DyRu_2Si_2$ (see figure 5 in [4]). For the magnetic field $H = 12.1$ kOe the diagram indicates only one magnetic phase in the temperature range 0–T_N.

For $ErRu_2Si_2$, the magnetic field causes a reduction of the Néel temperature T_N and a depression of the $R(T)$ maximum occurring at $T < T_N$. Both effects are due to the disappearance of the magnetic super zone gap. The magnetization curve of $ErRu_2Si_2$ [1] indicates that the magnetic field above $H_c = 2.5$ kOe destroys the antiferromagnetic order.

The field dependences of the electrical resistivity determined for $ErRu_2Si_2$ and $DyRu_2Si_2$ at $T = 2.0$ and 4.2 K are shown in figures 4(a) and 4(b). A strong decrease of the resistivity of $DyRu_2Si_2$ at $T = 2$ K below $H_{c1} \approx 1$ kOe up to $H_{c2} \approx 9$ kOe is observed. At $T = 4.2$ K the electrical resistivity increases linearly up to $H_{cr} \approx 9$ kOe. Such dependences agree with the field dependence of magnetization at low temperatures (see figure 2 in [4]). At both

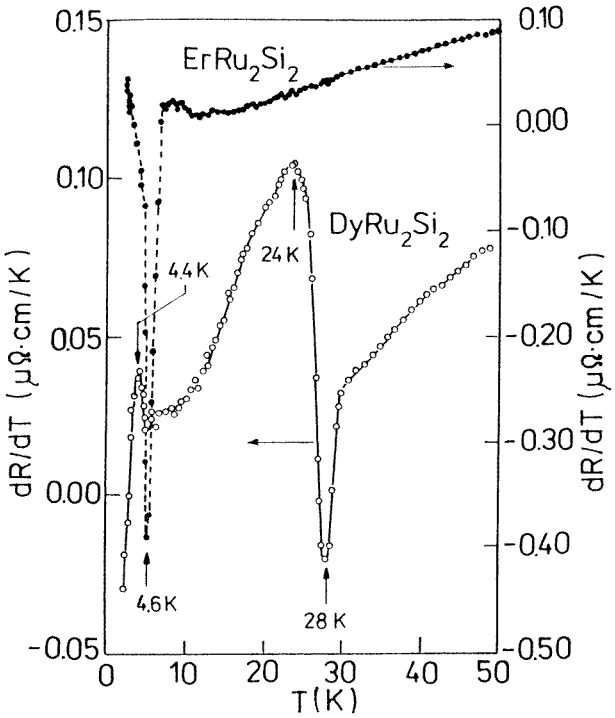

Figure 3. Temperature dependence of the differential resistivity dR/dT for $DyRu_2Si_2$ and $ErRu_2Si_2$ at low temperatures.

temperatures the magnetic field causes a decrease in resistivity but at $T = 2.0$ K this effect is large. The field dependence of the electrical resistivity of $ErRu_2Si_2$ runs at 2 as at 4.2 K. The electrical resistivity at $T = 2$ K is constant up to critical field $H_{cr} \approx 3$ kOe and then decreases. A similar dependence is observed at $T = 4.2$ K. In both temperatures the effect of the magnetic field is large and analogous to that observed at 2 K for $DyRu_2Si_2$. It suggests the existence of the square modulated magnetic structure below T_N which is confirmed by the neutron diffraction data for a single crystal [6]. At high temperatures, electron–phonon interaction is found to be dominant in resistivity R, which manifests itself in a linear increase in the $R(T)$ relation.

4.2. XPS valence band

The XPS valence bands (VBs) of the $DyRu_2Si_2$ and $ErRu_2Si_2$ compounds are presented in figures 5 and 6. The bands extend from the Fermi energy located at $E = 0$ to a binding energy of about 15 eV. The valence band spectra of both compounds have a characteristic maximum near the Fermi energy and several peaks located in the energy region between 3 and 11 eV. The positions of these peaks (equal to 3.9 and 10.5 eV for $DyRu_2Si_2$ and 5.0 and 8 eV for $ErRu_2Si_2$) correspond to the peaks observed in the valence band photoelectron spectra of pure dysprosium and erbium [13]. The measurement resolution was not good enough to observe the fine structure of electron emission of incompletely filled Dy and Er $4f^n$ shells.

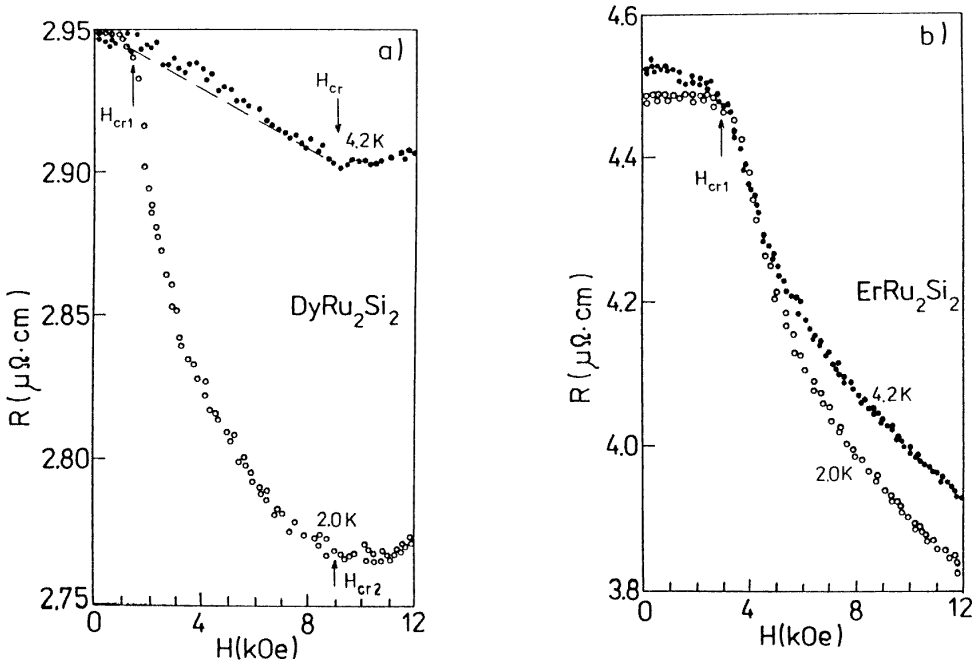

Figure 4. Magnetic field dependence of the electrical resistivity of (a) $DyRu_2Si_2$ and (b) $ErRu_2Si_2$ at $T = 2.0$ and 4.2 K.

4.3. Electronic structure

In figures 7 and 8 we present the calculated total and partial densities of states (DOSs) for $ErRu_2Si_2$ and $DyRu_2Si_2$. In the energy region between 0 and 5 eV a broad peak of 4d states of Ru atoms is observed. The Si state forms the narrow peak at $E = 9$ eV.

Results of calculation indicate that the density of states at the Fermi energy is actually connected with the d-state of Ru atoms. Similar results are obtained for isostructural URu_2Si_2 from the calculated electronic structure [14] as well as from the XPS spectra [15].

The calculated values of the densities of states are 2.31 [states eV^{-1}/cell] for $DyRu_2Si_2$ and 2.23 [states eV^{-1}/cell] for $ErRu_3Si_2$. They agree with the value of $N(E_F)$ for $ErRu_2Si_2$ determined from the electronic specific heat $\gamma = 60$ mJ mol^{-1} K^{-2} [6] equal to 2.55 [states eV^{-1}/cell].

As mentioned in section 3 the magnetic moments were calculated for two different models. In the first model we assumed the full hybridization of s (Si, Ru), p(Si), d(Ru) and f(Dy, Er) electrons while in the second one the Brooks model [10] was applied. The values of the magnetic moments are presented in table 1.

The value of the Dy magnetic moment in $DyRu_2Si_2$ was estimated as 10.1 and 9.6 μ_B fu^{-1} by the neutron diffraction measurement for a single crystal [3] and the magnetization measurement [4], respectively. The magnetic moment values for the Er in $ErRu_2Si_2$ are 9.07 [5] and 9.4 μ_B fu^{-1} [6], respectively. The magnetization measurement is a macroscopic method in which the localized 4f and delocalized s, p, d electrons are reflected. The neutron diffraction is a microscopic method which gives information on 4f electron. A comparison of values yielded by the magnetization and neutron diffraction methods suggests that the 4f electrons take no part in the hybridization in these compounds.

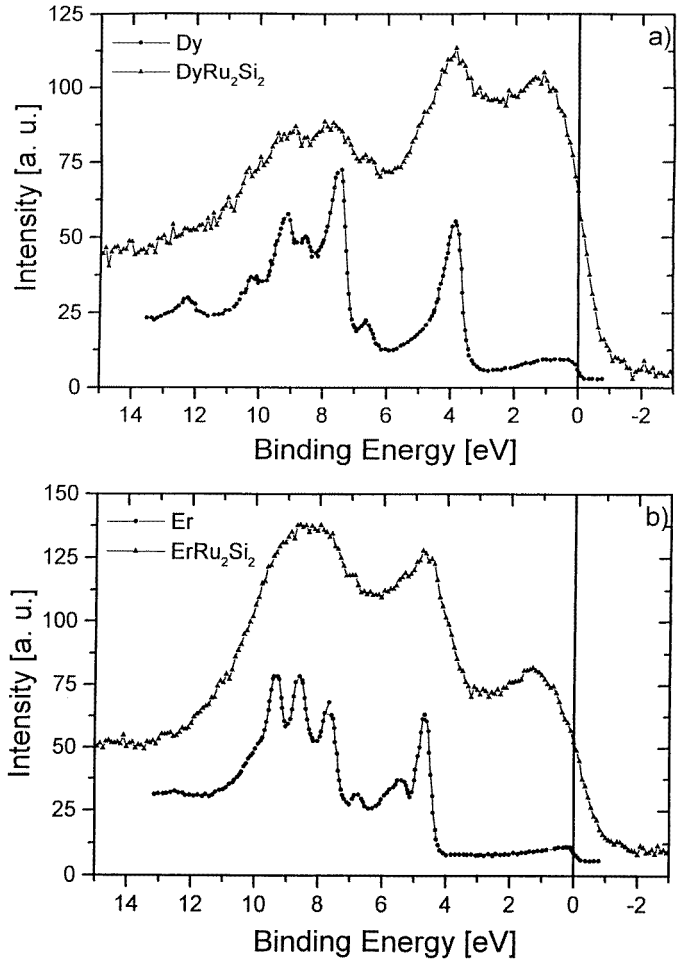

Figure 5. XPS valence band spectra for (a) $DyRu_2Si_2$ and (b) $ErRu_2Si_2$ and adequate spectra for metallic Dy and Er from [13].

Table 1. Value of the magnetic moments in $DyRu_2Si_2$ and $ErRu_2Si_2$.

	$DyRu_2Si_2$		$ErRu_2Si_2$	
	$\mu_{calc.}$ (μ_B)	$\mu_{obs.}$ (μ_B)	$\mu_{calc.}$ (μ_B)	$\mu_{obs.}$ (μ_B)
$R_{f\text{-}core}$	5(4f) + 0.12(spd) + 5(orb) = 10.12	10.1(2) ND	3(4f) + 0.07(spd) + 6(orb) = 9.07	9.07 ND
R_{spdf}	4.84 + 5(orb) = 9.84		2.51 + 6(orb) = 8.51	9.4 M
$Ru_{f\text{-}core}$	−0.02	9.6 M	−0.01	
Ru_{spdf}	+0.10		+0.065	
$Si_{f\text{-}core}$	0		0	
Si_{spdf}	+0.02		0	

In figures 7 and 8 we present the calculated electronic structure (DOS convoluted by Lorentzians of half-width 0.4 eV) where the proper photoemission cross sections were taken into account [11]. The shape of the calculated theoretical photoemission spectra is in good agreement with experimental data (figure 5).

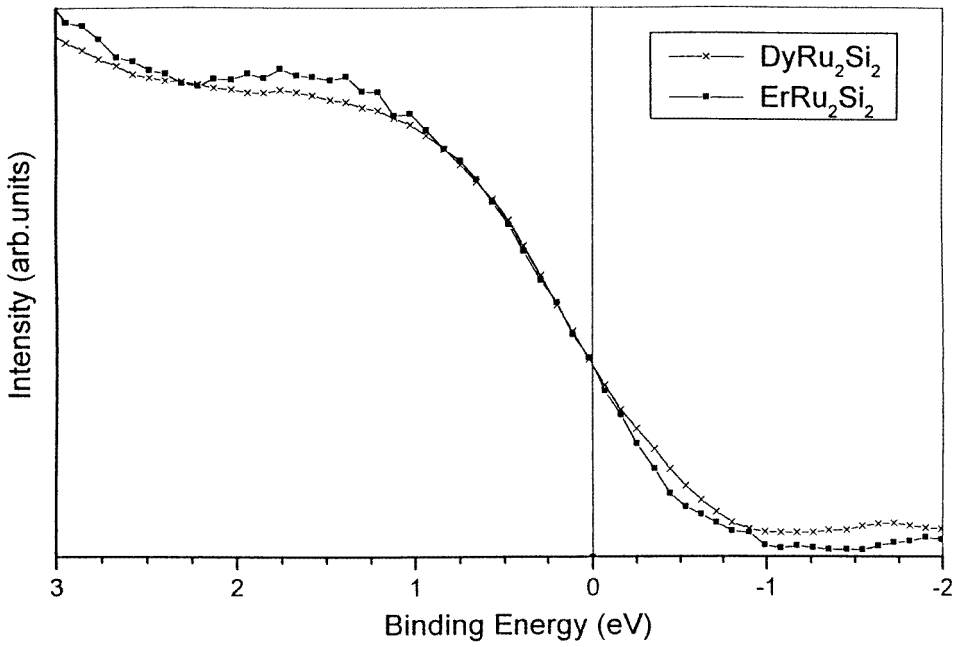

Figure 6. Valence band photoemission spectra of $DyRu_2Si_2$ and $ErRu_2Si_2$ taken at $h\nu = 40.8$ eV.

5. Discussion

The results of the electronic structure calculations which are in good agreement with XPS spectra indicate that the density of states at the Fermi level is formed by 3d electrons of Ru atoms. The calculated contribution of the band structure to the resistivity (equation (3)) indicates also that the model of Brooks *et al* [10] gives a good description of the electronic structure of $DyRu_2Si_2$ and $ErRu_2Si_2$ compounds.

The data obtained from the temperature and magnetic field dependence of the electrical resistivity allow for the following conclusions:

- the anomalies in $R(T)$ dependence at low temperatures correspond to the Néel or phase transition temperatures and are in good agreement with the values presented in the (H, T) magnetic phase diagrams of $DyRu_2Si_2$ [4] and $ErRu_2Si_2$ [16],
- the linear dependence of $R(T)$ at high temperature (above 100 K) indicates that electron–phonon interaction is dominant in resistivity R. The slope dR/dT indicates significant changes in the effective number of conducting electrons, thus subtle band overlap effects at the Fermi level. The slope dR/dT varies appreciably in different compounds, for example it is 0.069 $\mu\Omega$ cm K^{-1} for $DyCu_2Si_2$ and 0.063 $\mu\Omega$ cm K^{-1} for $ErCu_2Si_2$ [17] while for RNi_2Si_2 it is 0.345 $\mu\Omega$ cm K^{-1} for R = Dy and 0.306 $\mu\Omega$ cm K^{-1} for R = Er [18]. The dR/dT values determined in this work are for $DyRu_2Si_2$ 0.12 $\mu\Omega$ cm K^{-1} and for $ErRu_2Si_2$ 0.10 $\mu\Omega$ cm K^{-1}.

In the Bloch–Grüneisen transport theory the temperature dependence of R is related to the electron–phonon coupling constant λ by the relation [19]

$$\frac{dR}{dT} = \frac{8\pi^2}{h\omega_p^2} k_B \lambda_{tr} \tag{2}$$

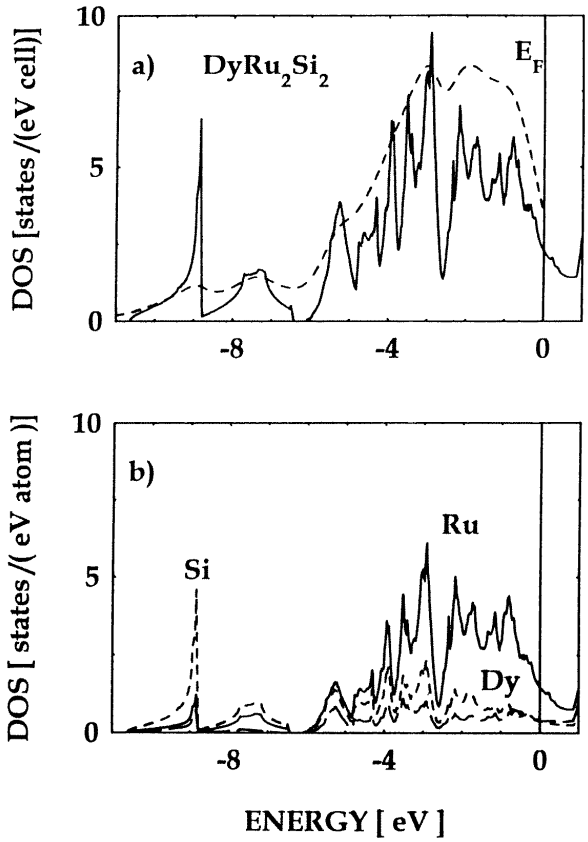

Figure 7. (a) The total density of states for paramagnetic $DyRu_2Si_2$. The Fermi level is located at $E = 0$ eV. The dashed curve presents the density of states convoluted by Lorentzians of half-width 0.4 eV and multiplied by cross sections [11]. (b) The contribution from Dy (s p d), Ru and Si to the total density of states.

where ω_p is the Drude plasma frequency given by the relation

$$\bar{h}^2\omega_p^2 = 4\pi e^2 N_F(0) v_F^2 \tag{3}$$

where $N_F(0)$ is the density of states at the Fermi level and v_F is the Fermi velocity. The values of $\mathrm{d}R/\mathrm{d}T$ and $N_F(0)$ for $ErRu_2Si_2$ and $DyRu_2Si_2$ compounds differ only a little which agrees with the relation that $\mathrm{d}R/\mathrm{d}T \sim 1/N_F(0)$.

The temperature dependence of electrical resistivity according to the Baber model [19] (which includes s–d scattering) is given by the formula [20, 21]

$$R(T) = R_0 + B(T - \alpha T^3) \tag{4}$$

where

$$\alpha = \left\{ \frac{\pi^2}{6} k^2 \left[3\left(\frac{1}{N}\frac{\mathrm{d}N}{\mathrm{d}E} \right)^2 - \frac{1}{N}\frac{\mathrm{d}^2N}{\mathrm{d}E^2} \right]_{E_F} \right\} \tag{5}$$

and N is the density state function, $\mathrm{d}N/\mathrm{d}E$ its first and $\mathrm{d}^2N/\mathrm{d}E^2$ its second derivate at the Fermi level. The calculated values of α coefficient are 0.31×10^{-7} and 0.37×10^{-7} for $DyRu_2Si_2$

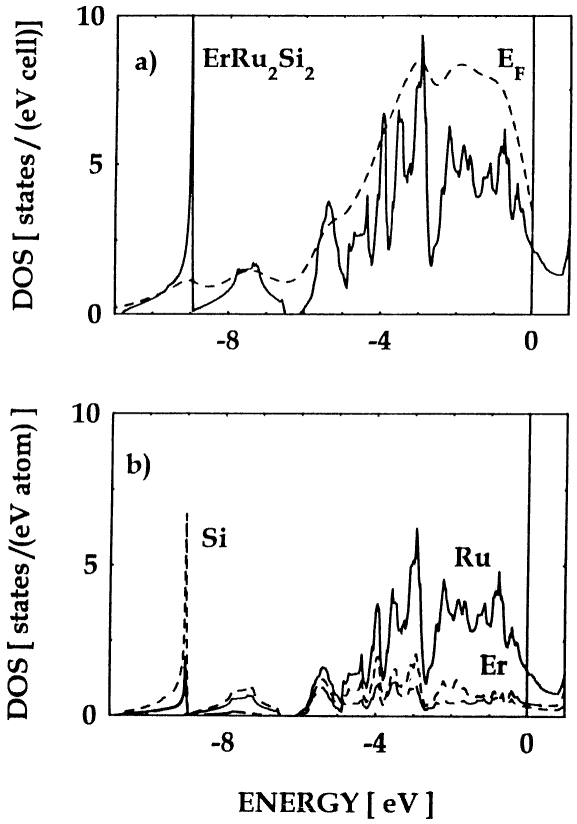

Figure 8. (a) The total density of states for paramagnetic $ErRu_2Si_2$. The Fermi level is located at $E = 0$ eV. The dashed curve presents the density of states convoluted by Lorentzians of half-width 0.4 eV and multiplied by cross sections [11]. (b) The contribution from Er (s p d), Ru and Si to the total density of states.

and $ErRu_2Si_2$ which indicates a small influence of the s–d scattering on the transport properties of these compounds. This is in good agreement with the determined dependence of $R(T)$.

Taking into consideration the R values measured at room temperature dR/dT and as well as the calculated band structure it is possible to estimate the electron mean free path (l) and transport electron–phonon coupling parameter (λ_{tr}).

The resistivity can be written as

$$R^{-1} = \tfrac{2}{3}e^2 N_F(0) v_F R. \tag{6}$$

The Fermi velocity v_F is calculated using the Fermi energy. For isostructural 1:2:2 compounds ($E_F = 8.28$ eV [22]) v_F is 5.4×10^7 cm s^{-1}. Assuming the same value of v_F for the $ErRu_2Si_2$ and $DyRu_2Si_2$ compounds the electron mean free values obtained using equation (4) are $l = 16.4$ Å for $DyRu_2Si_2$ and 16.0 Å for $ErRu_2Si_2$ at $T = 250$ K.

The values of plasma frequency estimated from equation (3) are $\hbar\omega_p = 5.3$ eV (Dy) and 5.2 eV (Er). The values of the electron–phonon coupling parameters λ_{tr} determined from equation (2) are 0.84 for $DyRu_2Si_2$ and 0.70 for $ErRu_2Si_2$.

The parameters estimated in this work are in good agreement with those determined for the RNi_2B_2C R = Dy, Er compounds [23]. The RNi_2B_2C compounds also crystallize in the tetragonal structure with the same $I4/mmm$ space group [24].

Acknowledgments

AS wishes to express his sincere appreciation to Professor A Hrynkiewicz for his help in the organization of our laboratory.

AJ thanks the State Committee for Scientific Research for financial support (project No 2 P03B 118 14).

References

[1] Slaski M, Szytuła A, Leciejewicz J and Zygmunt A 1984 *J. Magn. Magn. Mater.* **46** 114
[2] Bouvier M, Fraga G L F, Garnier A, Gignoux D, Schmitt D and Shigeoka T 1996 *Europhys. Lett.* **33** 647
[3] Kawano S, Shigeoka T, Iwata N, Mitani S and Ridwan 1993 *J. Alloys Compounds* **193** 303
[4] Andreani B, Fraga G L F, Garnier A, Gignoux D, Maurin D, Schmitt D and Shigeoka T 1995 *J. Phys.: Condens. Matter* **7** 1889
[5] Blaise A, Kmieć R, Malaman B, Ressouche E, Sanchez J P, Tomala K and Venturini G 1994 *J. Magn. Magn. Mater.* **135** 171
[6] Hamada R, Taleuchi T, Taniguchi T, Kawarazaki S and Miyako Y 1995 *J. Magn. Magn. Mater.* **140–144** 907
[7] Andersen O K and Jepsen O 1984 *Phys. Rev. Lett.* **53** 2571
[8] von Barth U and Hedin L 1972 *J. Phys. C: Solid State Phys.* **5** 1629
[9] Hu D and Langreth D C 1985 *Phys. Scr.* **32** 391
[10] Brooks M S S, Nordsom L and Johansson B 1991 *J. Phys.: Condens. Matter* **3** 2357
[11] Yeh J J and Lindau I 1985 *Atomic Data and Nuclear Data Tables* **32** 1
[12] Pinto R P, Amado M M, Salgueirosilva M, Braga M E, Sousa J B, Chevalier B and Etourneau J 1992 *J. Magn. Magn. Mater.* **104–107** 1235
[13] Cox P A, Lang J K and Baer Y 1981 *J. Phys. F: Met. Phys.* **11** 113
[14] Sandratskii L M and Kübler J 1994 *Solid State Commun.* **91** 183
[15] Suits J C 1976 *Phys. Rev.* B **14** 4131
[16] Gignoux D and Schmitt D 1997 *Handbook of Magnetic Materals* ed K H J Buschow (Amsterdam: Elsevier) p 376
[17] Cattaneo E and Wohlleben D 1991 *J. Magn. Magn. Mater.* **24** 197
[18] Barandiaran J M, Gignoux D, Schmitt D, Gomez Sal J C and Rodriguez Fernandez J 1987 *Phys. Rev.* B **36** 2920
[19] Baber W G 1933 *Proc. R. Soc.* A **158** 130
[20] Jones H 1956 *Handbook der Physik* vol 19 (Berlin: Springer) p 227
[21] Kowalczyk A and Jezierski A 1998 *J. Magn. Magn. Mater.* **188** 361
[22] Jarlborg T, Braun H F and Peter M 1983 *Z. Phys.* B **52** 295
[23] Bhatnagar A K, Rathnayaka K D D, Naugle D G and Canfield P C 1997 *Phys. Rev.* B **56** 437
[24] Siegrist T, Zandbergen H W, Cava R J, Krajewski J J and Peck W F Jr 1994 *Nature* **367** 254